DESIGN CASE STUDY

MMtC 2024-2025

Universidad Politécnica de Madrid

Alessandro Acuna

INDEX

List of Figures

List of Tables

1. Introduction

The objective of this work is to design the joint between a frame and a stringer made of composite material, which is attached to the skin of section 19. The connection will be achieved using a metal clip.

2. Problem Statement

The problem to solve with this case is the definition of the skin for a large airplane Rear Fuselage. The area to design will be limited by two frames two stringers.

The tasks are a DRW of the panel with schematic sections, the laminate in each area, the list of materials, the weight of the panel and the definition of the interfaces with frames.

Relating to the geometric data, the cylindrical surface radius is 4500 mm, the distance between frames plane is 550 mm and the circumferential pitch between stringer is 150 mm.

The material used will be unidirectional with a thickness of 0.184 mm.

These inputs are the aircraft surfaces and structural schemes, and the output would be a 3D Wire frame arrangement of the airframe elements on the aircraft surfaces.
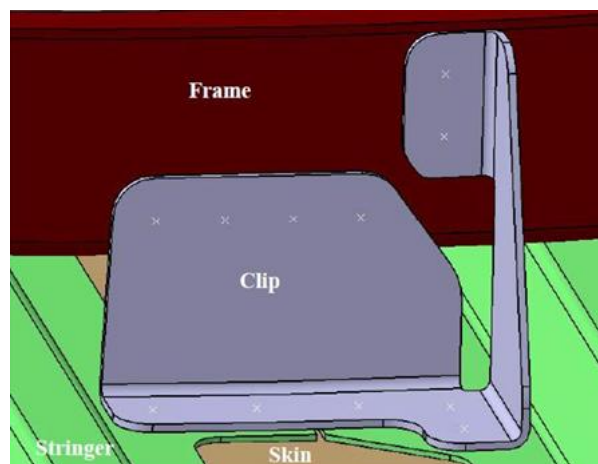
Figure 1. Schematic Figure to be Designed

3. Stringer Dimension

To size the stringer, we will first calculate the thickness of both the web and the falnges using the provided data:

- Layer thickness: 0.184 mm
- Number of web layers: 20 capas
- Number of flange layers: 10 capas

By multiplying the number of layers by the thickness of each layer, we can determine the total thickness:

Table 1. Web and Stringer Foot Laminate Thickness

Laminate Web	3,68 mm
Laminate Foot	1,84 mm

Regarding the mínimum radius of the stringer, its value will depend on the manufacturing process, as it can be fabricated using either a male or female mold. For each case, the minimm radius Rmin is determined as follows:

- If $Th < 2.5$ mm: (Rmin) the greater of: $2 * Th$ or 2 mm
- If $Th \geq 2.5$ mm: (Rmin) the greater of: Th or 5mm

We will choose the first option since the flange thickness t fis les tan 2.5 mm. As observed, manufacturing the stringer using a male mold results in a lower Rmin, which also satisfies the given condition Rmin>3mm. Therefore, we will select the following mínimum radius value with the corresponding tolerance due to the mold-based manufacturing process:

Table 2. Stringer Radius Dimension

R	4 mm	+/- 0.5 mm

To size the flange of the stringer, we will first calculate the values of the parameters s and p using the given nominal diameter:

D=4.8mm

- *Pitch: 5D≤p≤6D*
- *Edge distance: 4D≤s≤5D*

Substituting D=4.8 mm, we obtain the following values:

Table 3. s and p values

	Max (mm)	Min (mm)	Chosen	Tolerance
s	24	19.2	21	+/- 1mm

p	28.8	24	25	+/- 1mm

These values will be used for the flange dimensioning.

To calculate the mínimum distance of the rivets from the Edge of the stringer flange, we use the following formulas:

- *Shear joint:* $de = dm = 2.5 * D + 1\ mm$
- *Tension joint:* $de = 3D + 1mm$

These values define the minimum edge distances for the rivets based on the type joint:

Table 4. dm and dm_metal values

dm	>13 mm	14	+/- 1 mm
dm_{metal}	>10.6 mm	11.6	+/- 1 mm

3.1 Stringer Dimensions Calculation

Once we have obtained these values, we will proceed with the sizing of the stringer. To do this, we will calculate the maximum allowable width of the stringer flange, ensuring that even when the tolerances of the other components are at their maximum, the stringer does not interfere with the surrounding elements.

Table 5. Tolerances considered in the stringer design

Element	**Type**		**Tolerance**
Stringer	Dimension	S1	+/- 7%
		S2	+ 13% / -0%
		Alpha	+1º / -0º
		Theta	+1º / -0º
	Thickness	0 mm < t <10 mm	
		Web	+/- 8%
		Foot	+/- 8%
	Radius	Tool Side	+/- 0.5 mm
	Contour		+/- 0.75 mm
	Longitudinal	≤ 0.75 mm	+/- 0.25 mm

Firstly, we will calculate the máximum allowable web thickness, considering the following web tolerances:

- *Web:* $3.68 * 0.08 = 0.2944$ mm

- *S2:* $3.68 * 0.13 = 0.4784$ mm
- *Contour:* 0.75 mm

As a result, $tw_{max} = 3.68 + 0.2944 + 0.4784 + 0.75 = 5.2\ mm$

We will also consider the radius tolerances to determine the máximum allowable radius value:

- *Radio:* +/- 0.5

The maximum radius value is calculated as: $R_{max} = 4 + 0.5 = 4.5\ mm$

Similarly, we will consider the máximum allowable value for the reinforcement, which we will explain below. The máximum value for the reinforcement is 88.66 mm.
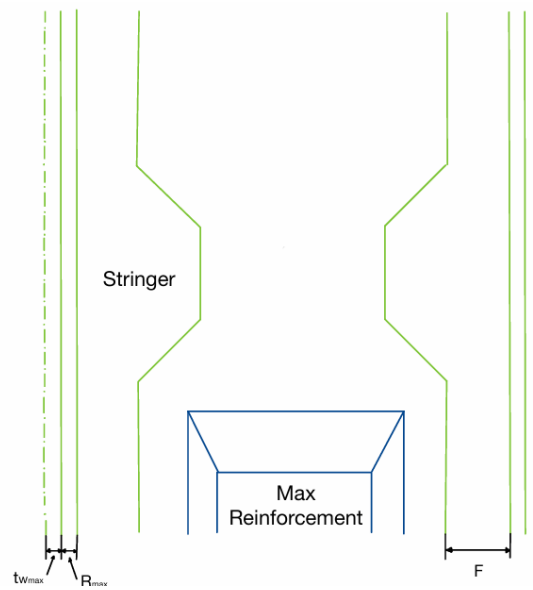
Figure 2. Schematic figure of the section

With the previous data, we will calculate the maximum allowable value for the stringer as follows:

$$F_{max} = \frac{150 - (tw_{max} + 2 * R_{max} + Reinforc_{max})}{2} = 23.3 \text{ mm}$$

Thus, the máximum allowable value for the stringer´s flange will be 23.3 mm. In our case, we have chosen a value that wnsures the dimensional tolerances are +/- 0.25 mm. This ensures the stringer fits correctly while accommodating any potential manufacturing variations.

Table 6. Fmax value

F_{max}	22 mm	+/- 0.25 mm

One we have calculated this dimensión, we will proceed to calculate the values of L1 and L.
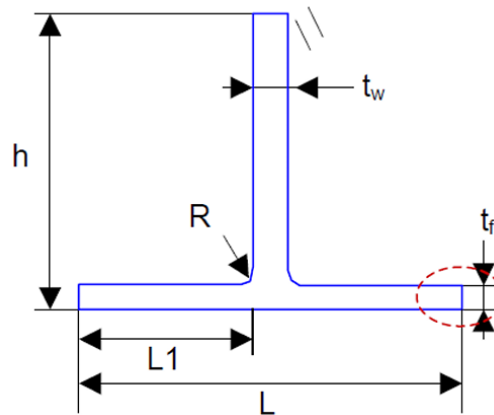
Figure 3. Stringer Schematic Section

Table 7. L1 and L values

L1	L1 = F + R	26 mm	+/- 0.25 mm
L	L= tw + 2xL1	55.68 mm	+/- 0.25 mm

3.2 Clip and Stringer Interface Dimension
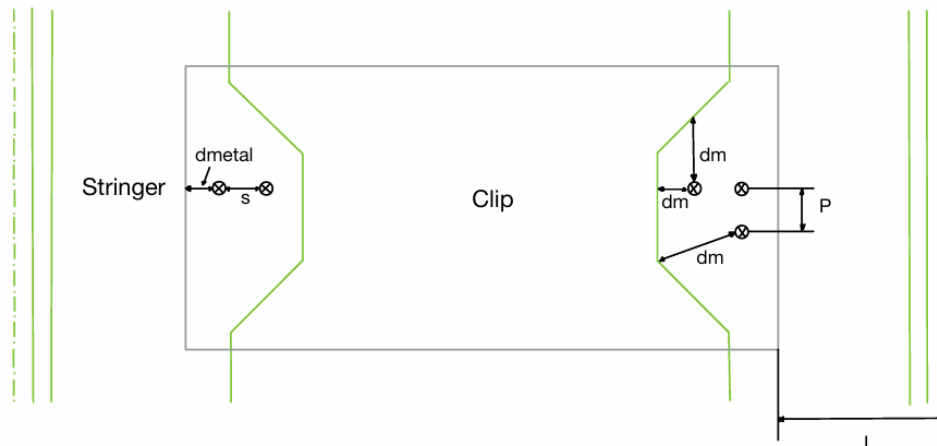
Figure 4. Schematic rivet position on the stringer

The distance between the stringer´s web and the clip, to avoid interference, must be greater than:

$$I_{min} = \frac{R_{max}}{2} + \frac{tw_{max}}{2} = 7.1 \ mm$$

We will choose the value I = 9 mm +/- 1mm

To calculate the distance between the web and the end of the protrusión, it will be equal to:

$$d_{web-edge} = I + dm_{metal} + s + dm = 55.6\ mm$$

4. Laminate

4.1 Skin Laminate

The skin laminate is made up of 9 layers, each with a thickness of 0.184 mm, giving a total thickness of 1.656 mm. This laminate has a thickness tolerance of +/-15 mm and a orientation tolerance of +/- 3º for the layers, as the lamination of the skin is carried out using a stacking process by AFP.

The lamination sequence must comply with the following:

- 2 layers at 0º
- 4 layers at +/-45º
- 3 layers at 90º

This stacking sequence ensures the laminate is symmetrical and balanced.

Additionally, as shown in the figure below, we have included the ECF layer and the Primer layer, which we will explain later.
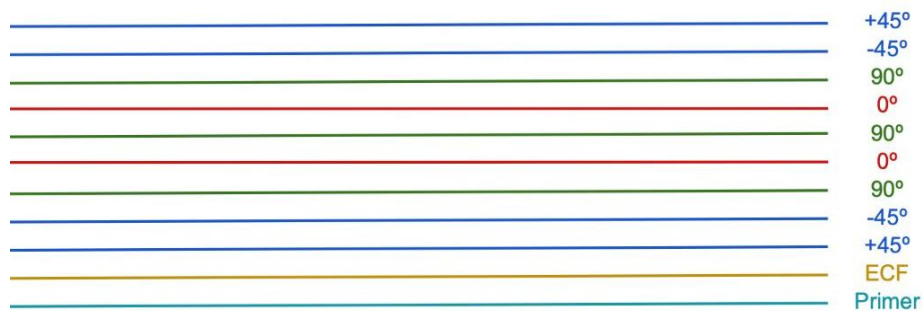
Figure 5. Skin Stacking Sequence

According to laminate theory, the layers oriented at +/-45º should be placed at the ends of the laminate to minimize coupling effects, improve damage tolerance, and prevent delamination due to accidental damage.

Placing the +/-45º layers at the outermost positions of the laminate helps distribute the loads more effectively and enhances the overall performance of the structure, particularly in terms of resistance to shear forces. This configuration ensures that the laminate can better withstand external forces and impacts, reducing the risk of structural failure due to delamination.

4.2 Stringer Laminate

The web and flange laminates are made up of 20 and 10 layers respectively, each one with a thickness of 0.184 mm. Giving a web total thickness of 3.68 mm and a flange total thickness of 1.89 mm.

The web lamination sequence must comply with the following:

- 10 layers at 0º
- 8 layers at +/-45º
- 2 layers at 90º

The flange lamination sequence must comply with the following:

- 5 layers at 0º
- 4 layers at +/-45º
- 1 layers at 90º

First, we will position the +/-45º plies on the outer zone of the stringer to improve damage tolerance. However, we will also place some of these plies in the center, so that at the separation of the web and the flangers, these layers are positioned in the outermost areas.

This arrangement will help enhance the overall strength and impact resistance of the stringer, ensuring that the external layers are well-protected against potential damage while also providing structural integrity at the critical interface between the web and flanges.

Regarding the intermediate layers, we need to avoid grouping more tan three layers in the same orientation. To achieve this, we will distribute the 0º layers in groups of three and two, separated by a 90º layer in between. This approach ensures the correct balance and avoids excessive concentration of layers in one orientation, which could affect the mechanical properties of the laminate.

Thu, our proposed lamination sequence is shown in the figure below, illustrating the layout of the layers with their respective orientations.
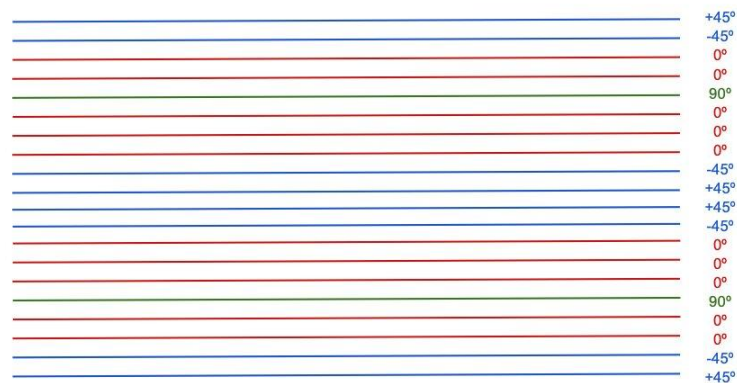
Figure 6. Stringer Stacking Sequence

5. Reinforcement

5.1 Dimensioning

The reinforcement for the fuselage skin panel has been dimensioned based on nominal measurements. It consists of a 100 mm reinforcement in the X-direction, positioned in the middle of the bay between the frames, and a 70 mm circumferential dimension between stringers, as illustrated in Figure 7.
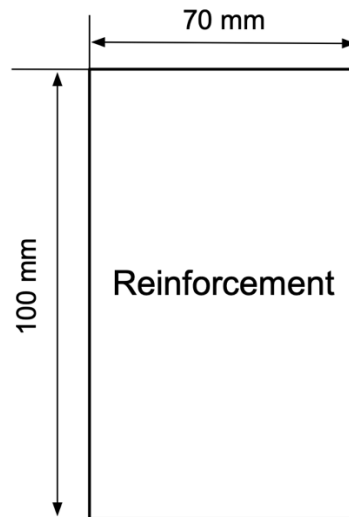
Figure 7. Reinforcement nominal dimensions

The addition of the reinforcement increases the local laminate thickness and requires a gradual transition between zones of different thickness. The ply drop-off slopes must adhere to the following design rules:

- In the main load direction (X-direction, along the stringers), the maximum slope ratio is 1:20.
- In any other direction, the maximum slope ratio is 1:10.

Considering these design criteria, the reinforcement dimensions are determined as follows:

The basic skin panel consists of 9 plies, while the reinforced skin thickness consists of 14 plies, resulting in 5 additional plies. Given the material's Cured Ply Thickness (CPT) of 0.184 mm, the additional thickness due to the reinforcement is calculated as:

$$Extra\ thickness = 5 * 0.184 = 0.92\ mm$$

In the main load direction, the reinforcement must extend beyond its nominal 100 mm length to allow for a smooth thickness transition. Using the 1:20 slope ratio, the extra length on each side is calculated as:

$$Extra\ length\ per\ side = 0.92\ x\ 20 = 18.4\ mm$$
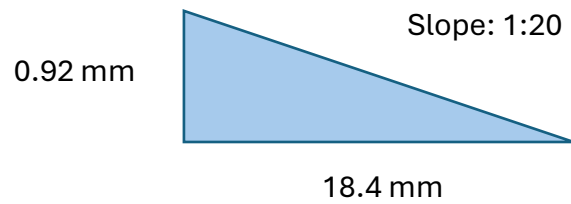
Thus, the total reinforcement length, including joggles becomes:

$$Total\ length = 100 + (2 * 18.4) = 136.8\ mm$$

In the circumferential direction, the extra width is calculated with the 1:10 slope ratio. The extra width on each side is:

$$Extra\ width\ per\ side = 0.92\ x\ 10 = 9.2\ mm$$
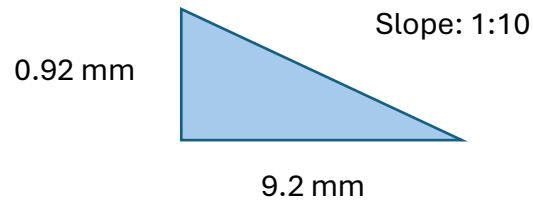
Resulting in a total adjusted reinforcement width of:

$$Total\ width = 70 + (2 * 9.2) = 88.4\ mm$$

The final reinforcement dimensions, including ply drop-off slopes and the tolerances applicable to the design of joggles, are illustrated in Figure 7 and Figure 8.

Table 8. Applicable tolerances to the design of the reinforcement

	Tolerance
Joggle return	+ 0.2 mm / - 0 mm
Joggle length	+ 0.2 mm / - 0 mm
Joggle depth	+ 0.4 mm / - 0 mm
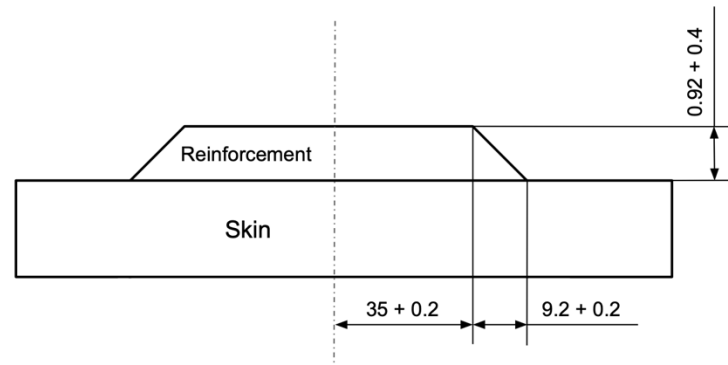
Figure 8. Reinforcement dimensions with joggles and tolerances
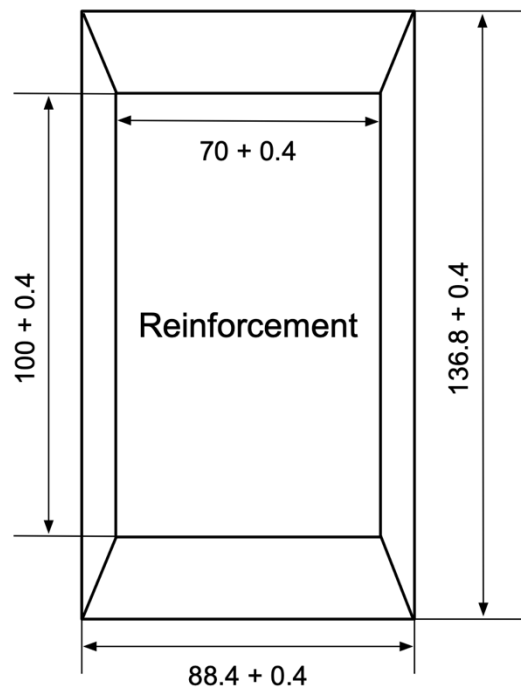
Figure 9. Reinforcement dimensions with joggles and tolerances

5.2 Stacking sequence

The provided skin data is as follows:

- Skin basic panel thickness: 9 plies (2/4/3)
- Skin reinforcement: 14 plies (2/8/4)

From this data, it can be concluded that the reinforcement adds five additional plies: four in the ±45° direction and one in the 90° direction.

There are various types of local reinforcements, Table 9 provides a comparison based on structural behaviour and manufacturability.

Table 9. Comparison of different types of reinforcements

Type of reinforcement	Load Transfer	Fatigue	Manufacturing
Interleaved reinforcement	Excellent	Excellent	Poor
Internal pad-up co-cured	Good	Good	Acceptable
External pad-up co-cured	Acceptable	Acceptable	Good
External pad-up co-bonded	Poor	Poor	Excellent

The three types of reinforcements were designed and compared, internal pad-up (Figure 9) external pad-up (Figure 10) and interleaved reinforcement (Figure 11). For both the internal and external pad-up, the extra plies from the reinforcement were added as a block on top of the skin, with a (+45º/-45º/90º/0º/90º/0º/90º/-45º/+45º) stacking sequence. In both cases, the pad up was designed to be symmetrical and balanced, with a (+45º/-45º/90º/-45º/45º) stacking sequence. However, this stacking sequence resulted in the complete laminate (skin laminate + reinforcement) not being symmetric and balanced, which violates one of the laminate design rules.

Additionally, another design rule states that no more than 3 or 4 consecutive plies should be dropped off without a continuous ply covering the dropped plies. This rule was not achievable in the the internal pad-up design, as the reinforcement consisted of 5 plies. To comply with this rule, the extra plies would need to be inserted between the skin plies to cover the dropped plies, which would result in an interleaved reinforcement.
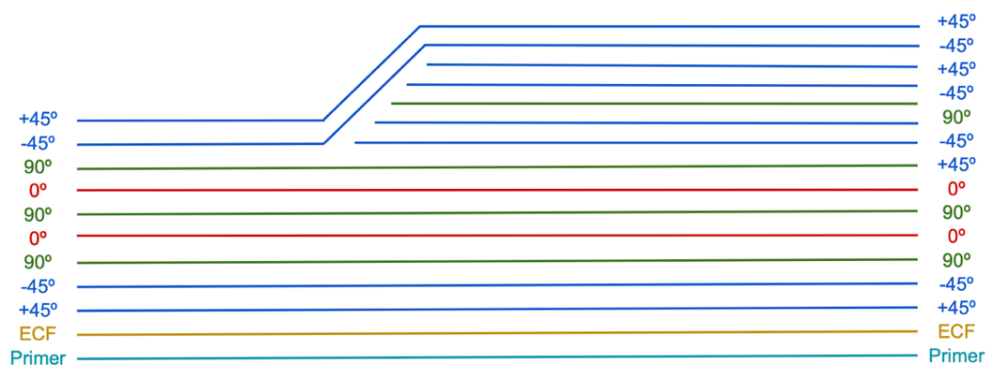
Figure 10. Internal pad-up
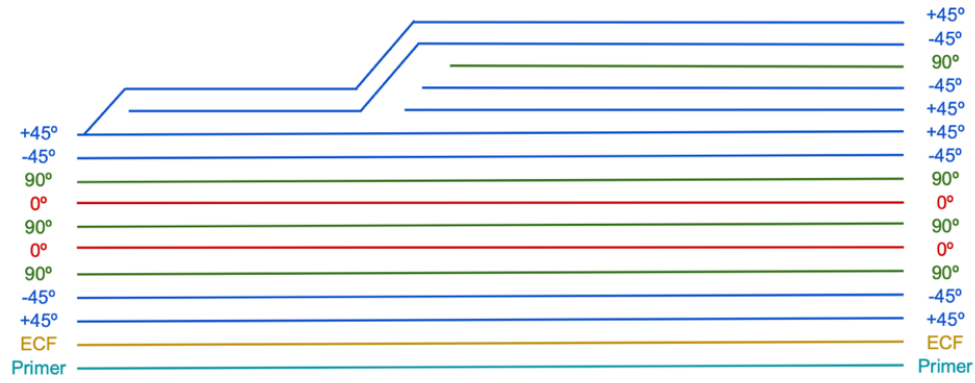
Figure 11. External pad-up

The manufacturing of the external pad-up is the most efficient among the different reinforcement methods since the reinforcement is laid up separately and then placed on top of the skin for co-bonding. However, as previously mentioned, the resulting complete laminate is neither balanced nor symmetric, which can lead to an inferior structural performance.

Considering the design rules of stacking sequences, plies drop-offs and reinforcements, the interleaved reinforcement was finally chosen as the most appropriate design, because it allowed for a symmetric and balanced complete laminate. This was achieved by inserting the extra 5 plies between the skin laminate plies, resulting in the following stacking for the complete laminate: (+45º/-45º/90º/-45º/+45º/0º/90º/90º/0º/+45º/-45/90º/-45º/+45º). Although this type of reinforcement slows down the manufacturing process, as the plies are laid up during the lay-up process of the complete laminate, it provides the best structural performance. Furthermore, having a symmetric laminate, prevents warping under thermal loading, and the balanced laminate avoids coupling between in-plane extension and shear behaviour.
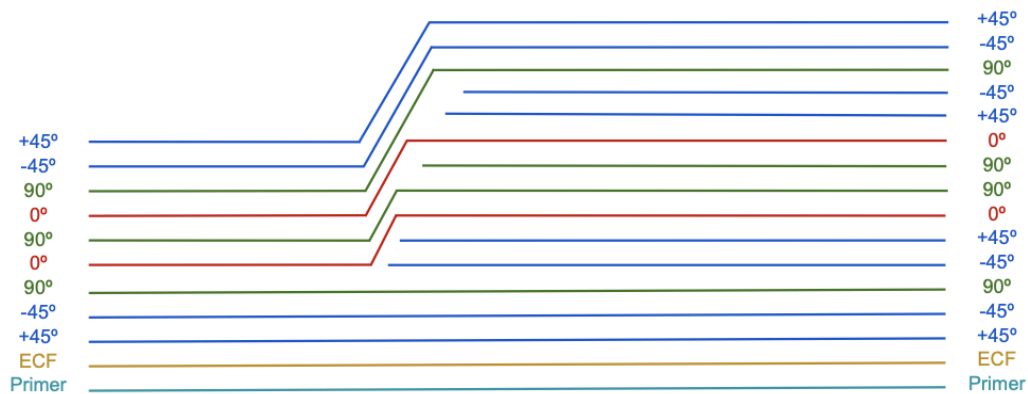
Figure 12. Interleaved reinforcement

6. Material Selection

Table 10. Properties Comparison HexPly®M21 and HexPly® M91

Properties	HexPly® M21	HexPly® M91
E_1 (Mpa)	150000	175000
E_2 (Mpa)	10000	9200
G_{12} (Mpa)	4000	5400
μ_{12}	0.25	0.25
t_{ply} (mm)	0.184	0.184
σ_{1Rt} (MPa)	3000	3940
σ_{2Rt} (MPa)	60.8	67.6
σ_{1Rc} (MPa)	1780	2050
σ_{2Rc} (MPa)	216	258
τ_{12R} (MPa)	69	95

HexPly® M21 and HexPly® M91 are two advanced composite materials used in aerospace and high-performance applications. Both materials exhibit excellent mechanical properties, but there are distinct differences that influence their selection depending on the specific requirements of a project.

HexPly® M21 has a longitudinal modulus of elasticity (E1) of 150 GPa, while HexPly® M91 offers a higher value of 175 GPa, indicating that M91 is stiffer in the fiber direction. However, in the transverse direction (E2), M21 performs slightly better with 10 GPa compared to 9.2 GPa for M91. Additionally, HexPly® M91 has a superior shear modulus (G12) of 5.4 GPa, compared to 4.0 GPa for M21, meaning it has better resistance to shear deformations. The Poisson's ratio (μ12) remains the same for both materials at 0.25, which indicates a similar lateral contraction behavior when loaded in the primary fiber direction.

Regarding strength properties, HexPly® M91 outperforms M21 in most aspects. It has a higher tensile strength in both fiber and transverse directions, with 3940 MPa in σ1RT and 67.6 MPa in σ2RT, compared to 3000 MPa and 60.8 MPa for M21, respectively. Compressive strengths follow a similar trend, where M91 has 2050 MPa (σ1RC) and 258 MPa (σ2RC), while M21 has 1780 MPa and 216 MPa. The shear strength (τ12R) of M91 is also significantly higher at

95 MPa compared to 69 MPa for M21. These values suggest that M91 provides greater structural integrity under both tensile and compressive loads.

Figure 13. HexPly® M21

Figure 14. HexPly® M91

In terms of laminate properties, the ABD matrix for both materials confirms that they are balanced, symmetrical, and specially orthotropic, ensuring no shear deformation under tension loads, no bending or twisting under in-plane loads, and no twisting deformation under bending loads. The ABD matrix for M91, however, shows generally higher stiffness values, reinforcing its superior mechanical performance.

Despite the higher performance of HexPly® M91, the selection of HexPly® M21 is based on a combination of factors beyond mechanical strength. One of the main reasons is manufacturability and processing. M21 has been widely used in aerospace applications due to its well-established processing methods, which offer reliable performance and ease of integration into existing production lines. Additionally, while M91 offers better mechanical properties, M21 provides a more favorable balance between performance and cost. The slight reduction in mechanical properties is acceptable for applications where extreme loads are not a primary concern, making M21 a more practical and cost-effective choice.

Ultimately, the choice of HexPly® M21 over HexPly® M91 is driven by the need for a proven, cost-effective, and manufacturable composite material that meets structural requirements without unnecessary complexity. While M91 offers superior mechanical properties, the

practical benefits of M21, including ease of processing and widespread aerospace adoption, make it the preferred option for this application.

7. Mechanical Joints

For the design of the panel, composed of the skin, two stringers, and two frames, the connection between the elements must be carefully considered. This connection is made using the clips previously mentioned. The connection to the frame is achieved with 6 fasteners, while the connection to the stringers is made with 5 fasteners (3 attached to the foot of one stringer and 2 to the foot of the other stringer).

In order to avoid purchasing various tools and types of rivets, all rivets will be of the same type. This also facilitates assembly for the factory workers.

The primary concern is the force parallel to the connection, as the joint will be subjected to shear stress. It will also experience tensile loads.

Given that this is a component that does not need to be disassembled for repairs in other areas, and with the goal of achieving the most durable connection possible, a permanent joint has been chosen.

The rivet that best suits these characteristics is a Hi-Lite type rivet, as it is a high-strength rivet used in applications where a durable and strong fastening is required. Hi-Lite rivets are designed to be lightweight and provide a strong joint in a variety of materials, such as metals or composite materials. Additionally, they are highly resistant to corrosion, making them suitable for harsh working environments, such as in the naval or aerospace industries.

A rivet from the **HSTR11** family will be used, which are rivets made of 6 AL 4V titanium alloy in the annealed state. This means that the composition of the alloy consists of 6% aluminium, 4% vanadium, and the remaining 90% is titanium.

The annealing process is a heat treatment that involves heating the material to a specific temperature and then slowly cooling it. The main purpose of annealing is to relieve internal stresses, improve ductility, and make the material easier to work or machine. In the case of titanium, annealing can also improve its corrosion resistance and modify its mechanical properties.

It features an ASTER recess, which is a system that facilitates more precise installation. The design of the recess in the rivet head allows for more accurate control over the deformation of the shank when the rivet is installed.

In Figure 14, we can see the diagram with the different parameters to be considered in the design of this Hi-Lite pin.
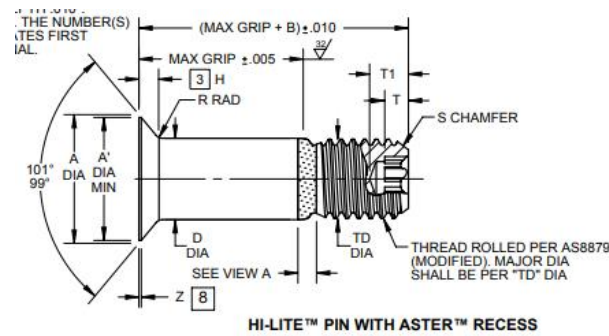
HI-LITE™ PIN WITH ASTER™ RECESS

Figure 15. Sketch of the rivet dimensions

This figure is associated with the table shown below to find the rivet that best suits the design.

Table 11. Rivet measurements

FIRST DASH NO.	PIN NOM DIA	A DIA	A' DIA MIN	B REF	D DIA		TD DIA	F	H	R RAD	Z MAX	S CHAMFER REF	THREAD MODIFIED	ASTER™ RECESS			DOUBLE SHEAR POUNDS MINIMUM	TENSION POUNDS MINIMUM
					WITHOUT ALUMINUM COATING	WITH ALUMINUM COATING								RECESS SIZE CODE	T1 DEPTH MAX	T DEPTH MIN		
5	5/32	.2612 .2564	.242	.280	.1635 .1630	.1635 .1625	.1595 .1570	.004	.0410 .0390	.025 .015	.010	1/32 X 37°	.1640-32 UNJC-3A	A5L-05	.118	.072	4,010	1,650
6	3/16	.3016 .2966	.270	.290	.1895 .1890	.1895 .1885	.1840 .1810	.005	.0470 .0450	.030 .020	.015	1/32 X 37°	.1900-32 UNJF-3A	A5L-06	.116	.069	5,380	2,000
7	7/32	.3403 .3355	.309	.305	.2182 .2177	.2182 .2172	.2100 .2070	.005	.0512 .0492	.030 .020	.015	1/32 X 37°	.2160-28 UNJF-3A	A5L-07	.117	.069	7,194	3,100
8	1/4	.3948 .3898	.363	.320	.2495 .2490	.2495 .2485	.2440 .2410	.006	.0610 .0590	.030 .020	.015	1/32 X 37°	.2500-28 UNJF-3A	A5L-08	.118	.069	9,300	3,700
10	5/16	.4739 .4689	.442	.380	.3120 .3115	.3120 .3110	.3060 .3020	.007	.0680 .0660	.040 .030	.015	3/64 X 37°	.3125-24 UNJF-3A	A5L-10	.127	.070	14,600	5,000
12	3/8	.5604 .5554	.529	.420	.3745 .3740	.3745 .3735	.3680 .3640	.008	.0780 .0760	.040 .030	.015	3/64 X 37°	.3750-24 UNJF-3A	A5L-12	.147	.087	21,000	7,200
14	7/16	.6680 .6620	.620	.485	.4370 .4365	.4370 .4360	.4310 .4260	.009	.0969 .0944	.050 .040	.022	3/64 X 37°	.4375-20 UNJF-3A	A5L-14	.196	.116	28,600	10,000
16	1/2	.7540 .7480	.706	.525	.4995 .4990	.4995 .4985	.4930 .4880	.010	.1068 .1043	.050 .040	.022	3/64 X 37°	.5000-20 UNJF-3A	A5L-16	.236	.139	37,300	13,500

The connection of the parts with the rivet is shown in the following figure. The supplier recommends using a collar or a nut for the assembly. Therefore, a trade-off is made to determine what is best to use in this case.
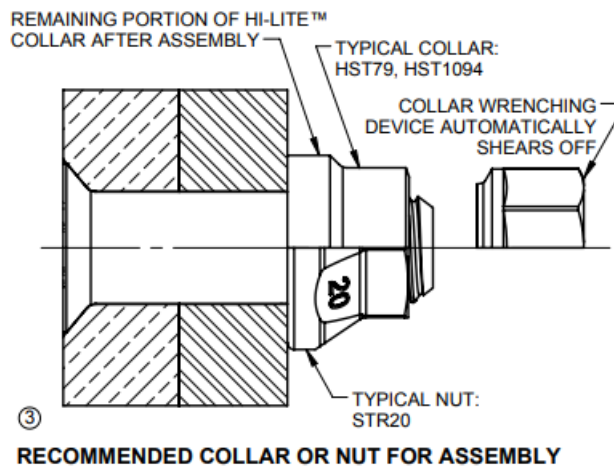

RECOMMENDED COLLAR OR NUT FOR ASSEMBLY

Figure 16. Typical collars or nut for the selected rivet

The collar is the part of the rivet that deforms or expands when installed. When pressure is applied, the collar bulges and locks into place, securing the two pieces being joined. It is generally the part of the rivet that forms the "head" or the opposite side of the installation.

The nut is the part that is placed at the opposite end of the collar and acts as an additional fastening means. In some Hi-Lite rivets, the nut may be a separate piece used to further secure the joint, providing additional fit or anchorage.

If accessibility in the installation area is limited, it is recommended to use a Hi-Lite rivet with a collar. A nut typically requires access to both sides of the material to place the nut on the opposite end and properly secure the fastening, which would be complicated if there is not enough space to work.

Finally, it was decided to place a collar.

To determine the rivet dimensions, the thickness of each layer to be riveted must be taken into account. The maximum height of the rivet head is calculated by summing the thicknesses of the 9 layers of skin, 1 layer of bronze mesh, and 1 layer of primers.

$$s_1 = 9 * 0.184 + 1 * 0.2 + 1 * 0.1 = 1.956 \ mm$$

$$H \leq {}^2\!/_3 \, s_1 \rightarrow H \leq {}^2\!/_3 * 1.956 \rightarrow H \leq 1.304 \ mm$$

Given that the design requirement for the rivet specifies a nominal diameter of 4.8 mm, it is necessary to consult the table above to identify the rivet that most closely matches this value, bearing in mind that the values in Table 10 are provided in inches.

$$\emptyset = 4.8 \ mm * \frac{1 \ in}{25.4 \ mm} = 0.18897 \ in$$

Therefore, a rivet smaller than this size should be selected, one that most closely approximates it. That rivet is number 6, which has a diameter of 0.1885 in.

$$\emptyset = 0.1885 \ in * \frac{25.4 \ mm}{1 \ in} = 4.788 \ mm$$

$$H = 0.045 \ in * \frac{25.4 \ mm}{1 \ in} = 1.143 \ mm$$

This rivet satisfies the diameter and head height requirements, as $H = 1.143 \ mm < 1.304 \ mm$

For a double shear joint, the following conditions must be satisfied:

$$0.4 < s_{1-2-3}/D < 1 \ ; S_T/D \leq 4.5$$

1. Skin:

$$s_1 = 1.956 \ mm \rightarrow \frac{s_1}{D} = \frac{1.956 \ mm}{4.8 \ mm} = 0.4075 \rightarrow It \ satisfies \ the \ condition.$$

2. Stringer:

$$S_2 = 10\ plies * 0.184\frac{mm}{ply} + 0.125\ mm\ (glass\ fiber) = 1.965\ mm$$

$$\frac{S_2}{D} = \frac{1.965\ mm}{4.8\ mm} = 0.41 \rightarrow It\ satisfies\ the\ condition.$$

3. Clip:

$$S_3 = clip\ thickness \rightarrow Estimated: 2.3\ mm$$

$$S_T = S_1 + S_2 + S_3 = 1.956 + 1.965 + 2.3 = 6.221\ mm$$

$$\frac{S_T}{D} = \frac{6.221\ mm}{4.8\ mm} = 1.296 < 4.5 \rightarrow It\ satisfies\ the\ condition.$$

The measurement of the selected rivet are:

- Nominal diameter: 4.8 mm

- Total length: $L = \frac{4}{16}in * 25.4\frac{mm}{in} + 0.29\ in * 25.4\frac{mm}{in} = 13.716\ mm$

- Head diameter: $\emptyset_h = 0.2966 * 25.4\frac{mm}{in} = 7.53\ mm$

- Head height: $H_h = 1.143\ mm$

Between the two types of collars defined by the manufacturer for the selected rivet (**HST79** and HST1094), it was decided to choose the first one because it is made of a stainless steel and aluminium alloy, which has better corrosion resistance properties than the other collar made of stainless steel. The following figure shows the collar design. The one with a precise diameter for the pin used was chosen ($\emptyset = 0.196\ in = 4.97\ mm; L = 0.385\ in = 9.78\ mm$).
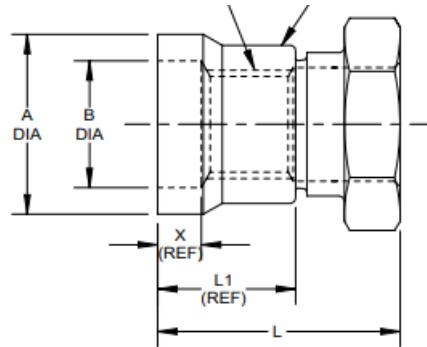

Figure 17. Collar Dimensions

To dimension the clip, the rivet spacing calculated previously must be considered.

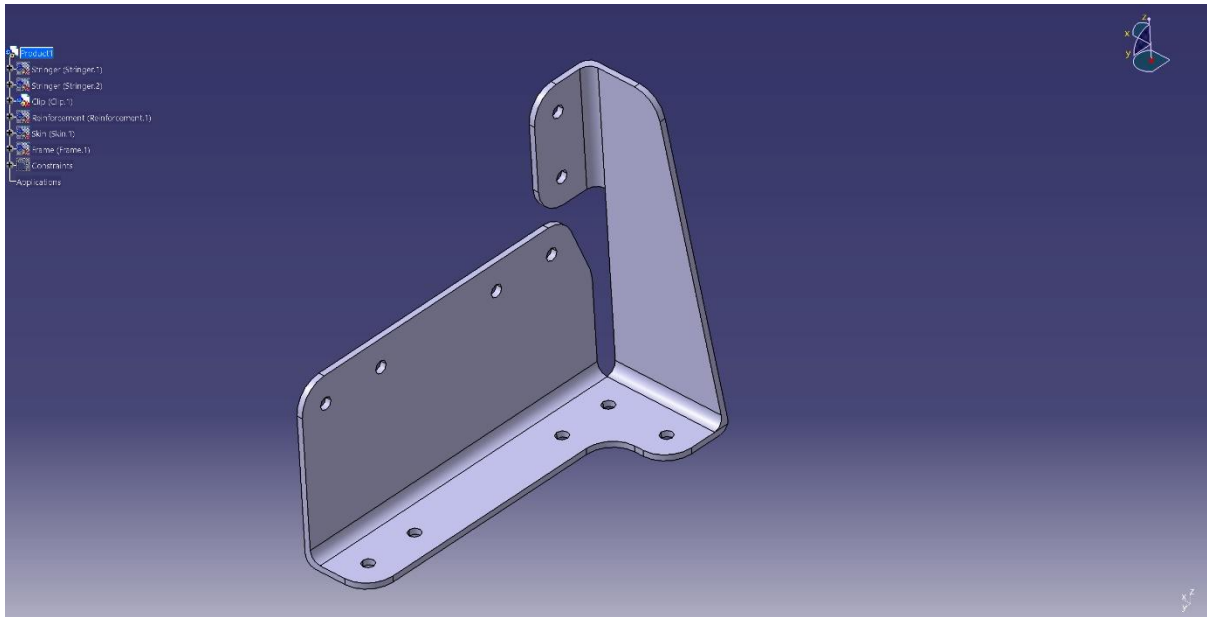p=25 mm.

s=21 mm.

Given that the clip is made of aluminium, a metal, the minimum distance to the edge will be:

$$D_{min} = 2D + 1\ mm = 2 * 4.8 + 1 = 10.6\ mm$$

With the calculated dimensions, the geometry of the clip has been created in Catia.

Figure 18. Clip geometry made in Catia

8. Strike protection

The lightning strike protection system outlined in the document focuses on ensuring the aircraft's structural integrity and safety during lightning strikes. The skin of the aircraft, located in section 19, is particularly vulnerable to lightning strikes, classified as a Zone 2A area. To address this, the system emphasizes low weight, corrosion avoidance, and high durability.

The protection system leverages materials with excellent electrical conductivity to efficiently dissipate lightning currents. This is crucial for preventing damage to the aircraft's structure. Additionally, high thermal conductivity helps prevent localized overheating during strikes, which can cause significant damage to composite materials. The chosen materials are also durable, resistant to wear, fatigue, and environmental degradation over time, ensuring long-term reliability.

When considering lightning strike protection for aircraft, materials like copper mesh are often chosen due to their excellent electrical conductivity, which ensures efficient dissipation of lightning currents. This is crucial for preventing damage to the aircraft's structure. Here's a detailed explanation of why copper mesh is a preferred choice, along with relevant tables from the document:

Electrical Conductivity and Thermal Conductivity

Copper mesh offers excellent electrical conductivity, which is essential for safely dissipating lightning currents. Additionally, its high thermal conductivity helps prevent localized overheating during strikes, which can cause significant damage to composite materials.

Durability and Corrosion Resistance

Copper mesh is durable and resistant to wear, fatigue, and environmental degradation over time. It also performs well in humid or saline environments, reducing maintenance needs and ensuring the structural integrity of the aircraft.

Flexibility and Proven Performance

Copper mesh is suitable for curved aircraft sections, providing flexibility where needed. It has been widely used and tested in aerospace applications for reliable lightning protection, offering robust mechanical support when integrated into composite materials.

The following table compares different materials for lightning strike protection:

Table 12. Different materials for strike protection

Material	Conductivity	Weight	Cost	Durability	Galvanic corrosion	Reparation	Density (g/cm3)
Bronze Mesh	🟨	🟨	🟨	🟩	NO	🟥	8.73
Copper Mesh	🟩	🟩	🟥	🟩	NO	🟥	8.96
Copper Foil	🟩	🟩	🟥	🟨	NO	🟨	8.96
Expanded copper foil	🟩	🟨	🟥	🟨	NO	🟥	8.96
Aluminium Mesh/Foil	🟨	🟥	🟩	🟥	YES	🟨	2.7

While aluminum mesh or foil is lighter, it poses a risk of galvanic corrosion, which can be detrimental in certain environments. Copper mesh, despite being heavier, offers superior durability and resistance to corrosion, making it a safer choice for critical applications like lightning strike protection.

9. Corrosion protection

Corrosion in aircraft is a significant concern as it can compromise the structural integrity and safety of the aircraft. There are several types of corrosion, but galvanic corrosion is particularly noteworthy due to its potential for rapid damage.

What is Corrosion?

Corrosion is a natural process where metals deteriorate due to interactions with their environment. In aircraft, this often involves exposure to moisture, salt, and other contaminants that accelerate the corrosion process. Corrosion can lead to a weakening of the aircraft's structure, potentially causing safety hazards and increasing maintenance costs.

Galvanic Corrosion

Galvanic corrosion, also known as bimetallic corrosion, occurs when two different metals or alloys come into direct contact in the presence of an electrolyte, typically moisture. This contact creates a galvanic cell, where one metal acts as the anode (corroding) and the other as the cathode (protected). The anode metal will degrade faster than if it were alone, while the cathode remains relatively unaffected.

Causes of Galvanic Corrosion in Aircraft

1. Dissimilar Metals: The use of different metals in aircraft construction, such as aluminum and steel, can lead to galvanic corrosion when these metals are in contact.

2. Moisture: The presence of moisture acts as an electrolyte, facilitating the galvanic reaction.

3. Environmental Factors: Exposure to saltwater environments or high humidity accelerates the process.

Prevention of Galvanic Corrosion

To prevent galvanic corrosion, aircraft manufacturers and maintenance teams use several strategies:

1. Material Selection: Choosing materials that are less prone to galvanic corrosion, such as using similar metals for components that will be in contact.

2. Insulation: Placing insulating materials between dissimilar metals to prevent direct contact.

3. Coatings: Applying protective coatings to metals to prevent moisture from reaching the surface.

4. Regular Maintenance: Regular inspections and maintenance to detect and address corrosion early.

Impact on Aircraft Safety

Galvanic corrosion can significantly compromise aircraft safety by weakening structural components. It is essential to identify and address corrosion issues promptly to ensure the airworthiness of the aircraft. Regular inspections and the use of advanced coatings and materials are critical in preventing this type of corrosion.
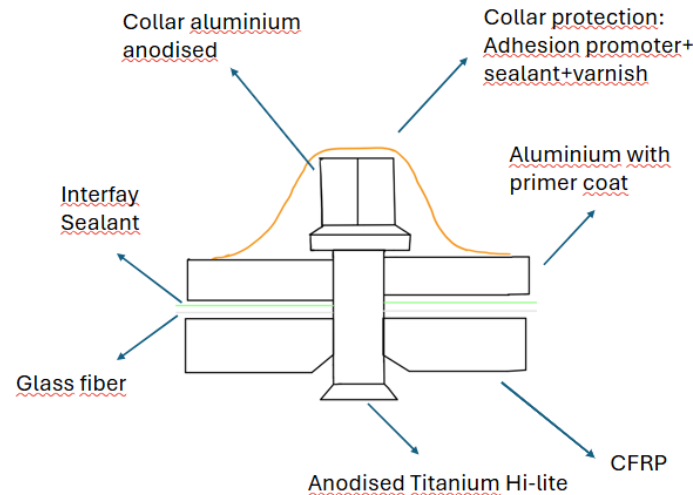
Figure 19. Diagram of different parts between the rivet and CFRP

Aircraft Component Protection

The diagram details how corrosion protection is implemented in a mechanical joint consisting of multiple materials, such as aluminum, titanium, and composite materials like CFRP (Carbon Fiber Reinforced Polymer). Key protective measures include:

1. Anodized Aluminum Collar: The aluminum collar is anodized to create a protective oxide layer that resists corrosion.

2. Sealants and Adhesives: Interfay sealants are applied between layers to prevent moisture ingress, which acts as an electrolyte.

3. Glass Fiber Layer: A glass fiber layer is used as an insulating barrier between dissimilar materials to prevent direct contact.

4. Primer Coatings: Aluminum surfaces are coated with primers to enhance adhesion and provide an additional protective layer.

5. Anodized Titanium Fasteners: Titanium fasteners are anodized to resist corrosion and ensure compatibility with surrounding materials.

6. Collar Protection: The collar is further protected with adhesion promoters, sealants, and varnish to enhance durability.

Material Properties for Corrosion Protection

The table below summarizes the materials used for corrosion protection, their thicknesses, and densities:

Table 13. Thickness and density of different materials used to avoid corrosion

Material	Thickness (mm)	Density (g/cm3)
Glass fiber	0,125	2,6
Sealant and adhesives	0,1	1-1,5
Primers and paints	0,1	1,2-1,8

Layered Structure

The layered structure of the joint is designed for optimal protection against corrosion while maintaining mechanical strength. The total thickness of the assembly is calculated as 6.296 mm, with contributions from:

This multi-layered approach ensures that each component contributes to both structural integrity and corrosion resistance.

Table 14. Thickness of every part in the join of the stringer, skin and clip

Layers	Thickness (mm)
Skin	1,656
Stringer	1,84
Clip	2,3
ECF	0,2
Glass fiber	0,1
Sealant and adhesives	0,1
Primers and paints	0,1
TOTAL	6,296

10. List of materials and weight

To calculate the weight of the materials, the various components were first designed individually in CATIA, using the dimensions referenced in the previous paragraphs. Subsequently, using the "Measure Inertia" feature, the density of the materials was assigned based on the values obtained from the datasheets, the densities are shown in the following table.

Table 15. Total volume, density and weight of stringer, skin, clip and reinforcement

Component	Volume (m³)	Density (kg/m³)	Weight (kg)
Stringer	1,34e-4	1580	0,212
Skin	2,123e-4	1580	0,335

Clip	4,135e-5	2710	0,112
Reinforcement	8,678e-6	1580	0,014
Rivets	2,829e-7	4430	0,001
ECF	1,64e-5	2600	0,043
CORROSION PROTECTION	2,46e-5	3800	0,093

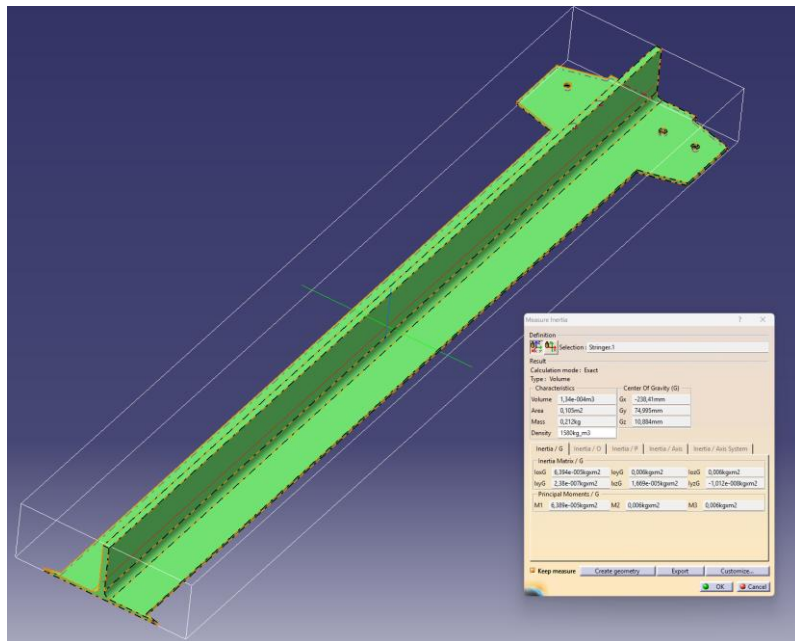The following image, Figure 20, illustrates an example of the stringer component:

Figure 20. Measure Mass of Stringer

The table below provides a summary of all material components, indicating the quantity and total weight of each item, so the total weight of the assembly is 1,032 kg.

Table 16. Total Weight and Quantity of the assembly

Item	Description	Quantity	Material	TOT (kg)
1	Stringer	2	CFRP	0,424
2	Skin	1	CFRP	0,335
3	Clip	1	Al	0,112
4	Reinforcement	1	CFRP	0,014

5	Rivets	11	Ti6Al4V	0,011
6	ECF	1	Cu	0,043
7	CORROSION PROTECTION	1	Glass Fiber	0,093
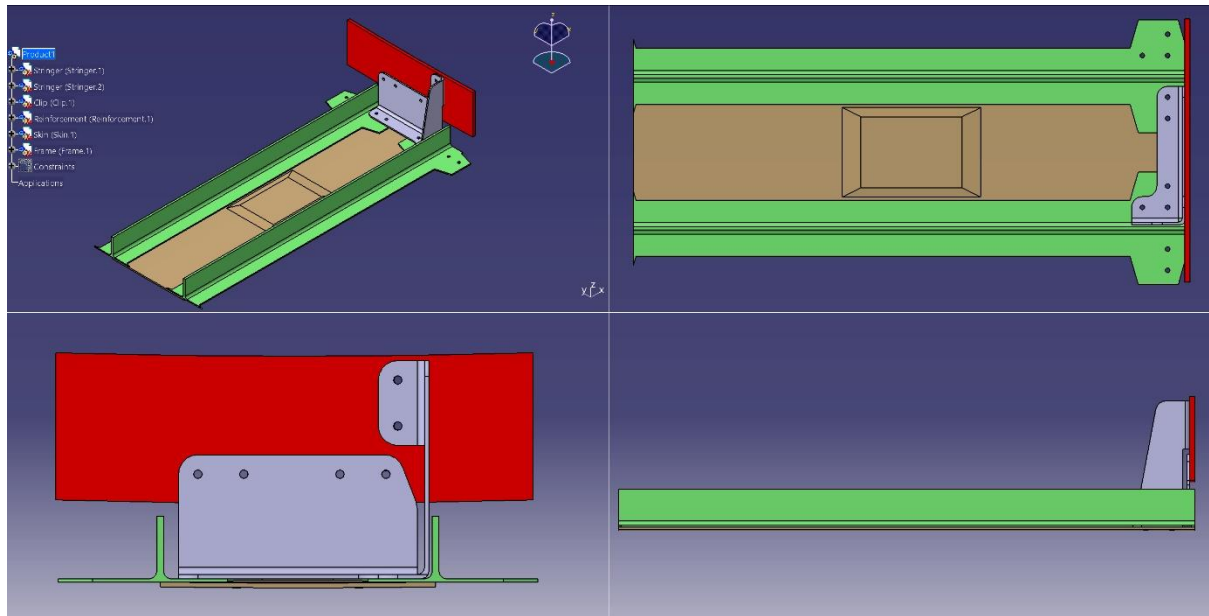
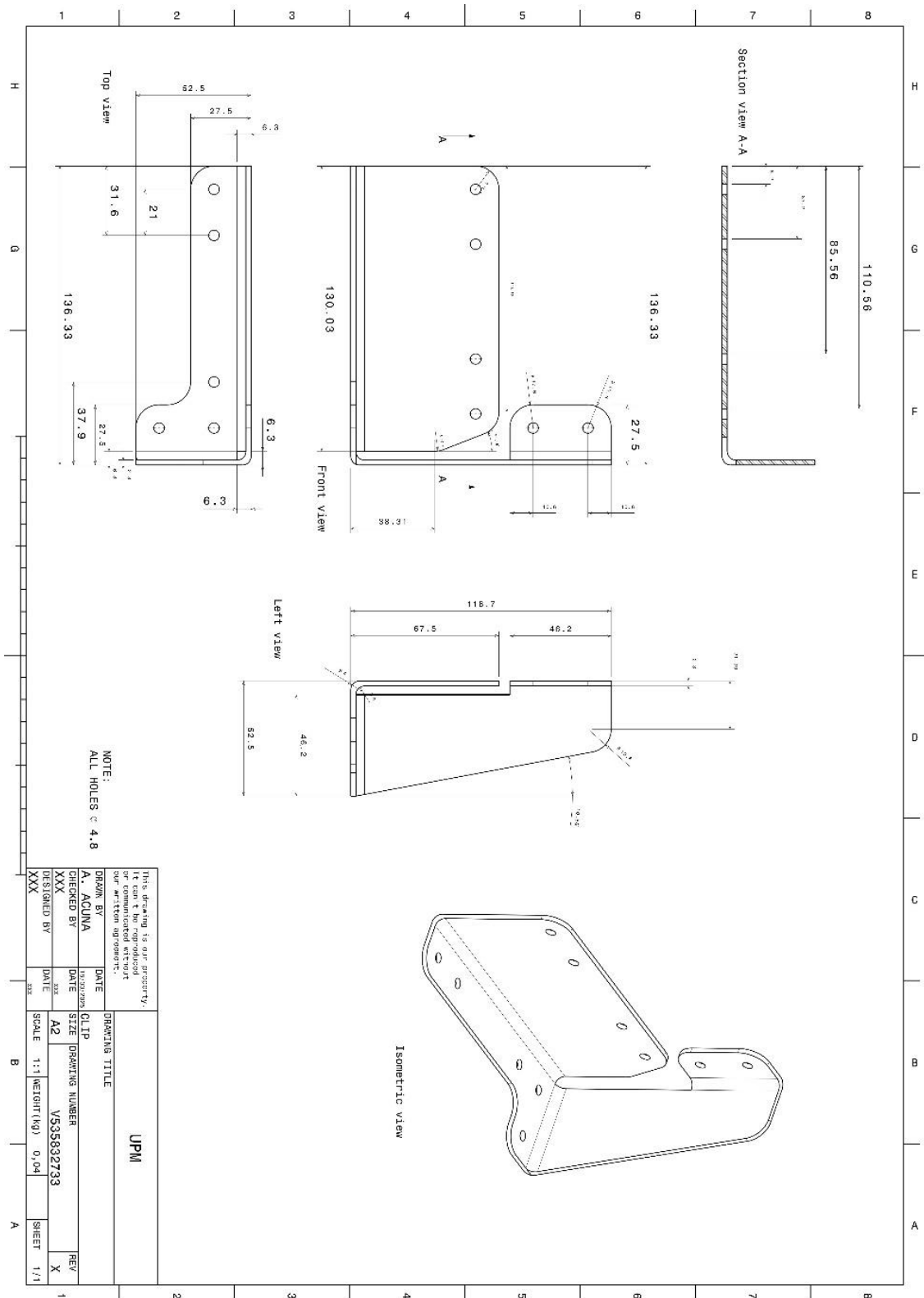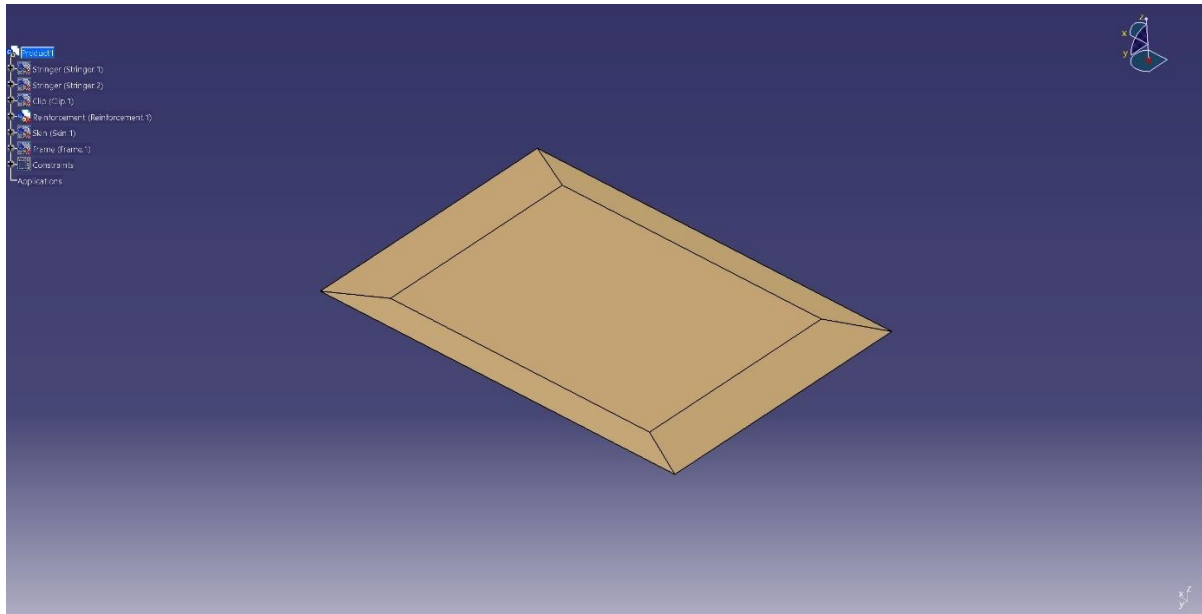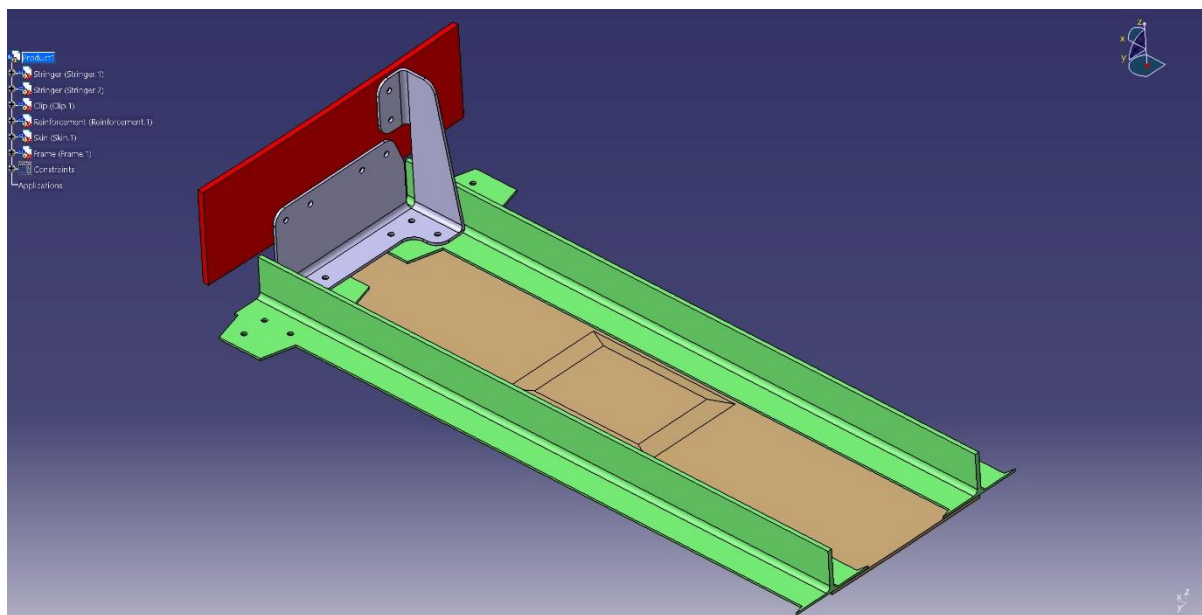*Figure 21: Assembly with all the components*

APPENDIX

Figure A1. Drawing of the clip

Figure A2. CATIA model of the reinforcement

Figure A3. CATIA model of the whole assembly

Figure A4. Drawing of the Stringer
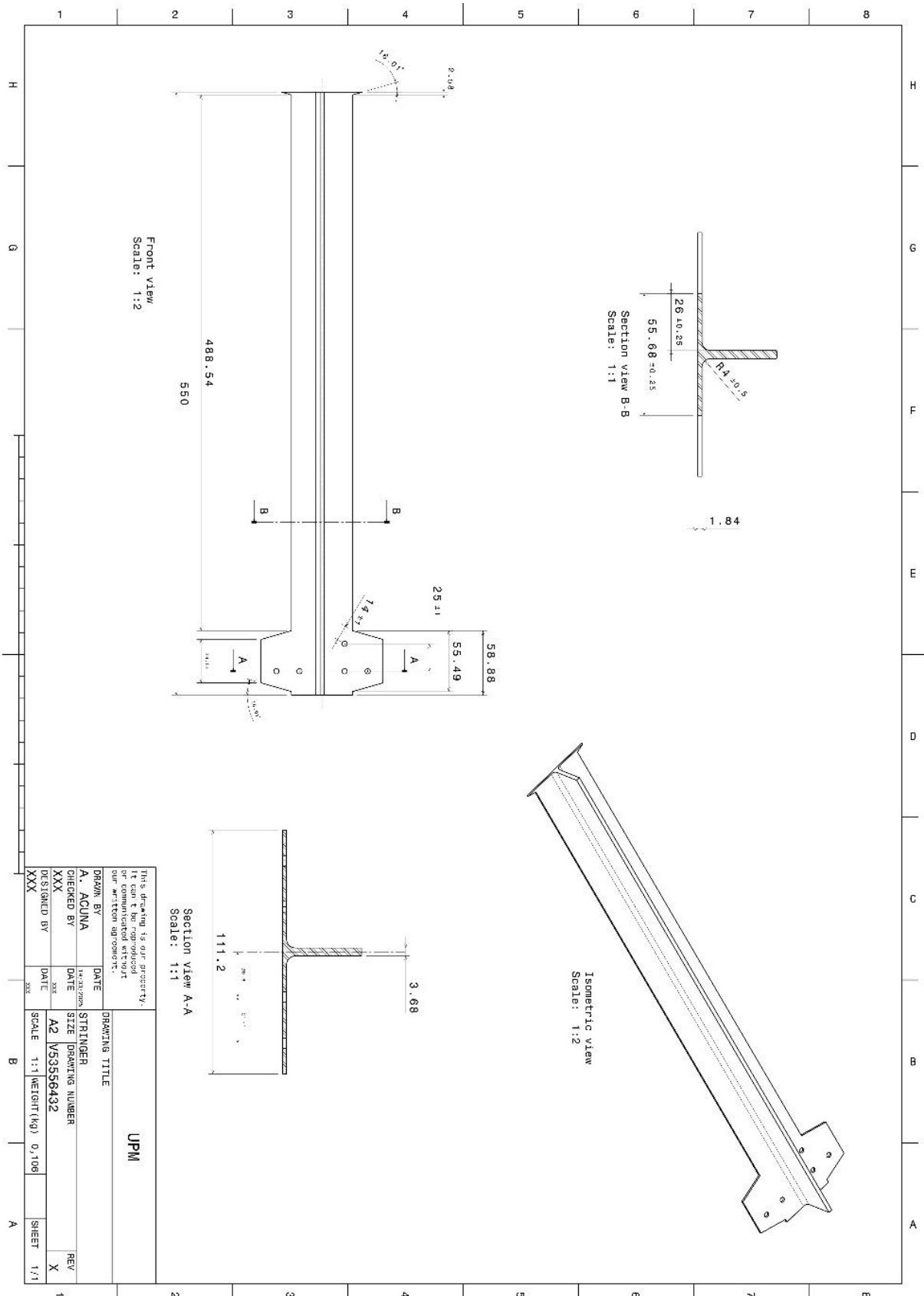
REFERENCES

[1] HSTR11

https://www.lisi-aerospace.com/en/configurator-drawing-download/HSTR11/

[2] HST79

https://www.lisi-aerospace.com/en/configurator-drawing-download/HST79/

[3] HST1094

https://www.lisi-aerospace.com/en/configurator-drawing-download/HST1094/